JOURNAL OF Applied Polymer SCIENCE

Preparation and Characterization of Acrylic Polymer Nanocomposite Films Obtained from Aqueous Dispersions

Catarina Carneiro,[1,2] Ricardo Vieira,[2] Adélio M. Mendes,[2] Fernão D. Magalhães[2]

[1]CIN — Corporação Industrial do Norte, S.A., Avenida Dom Mendo 831, Apartado 1008, 4471-909 Maia, Portugal

[2]LEPAE — Departamento de Engenharia Química, Faculdade de Engenharia, Universidade do Porto, Rua Dr. Roberto Frias, 4200-465 Porto, Portugal

Correspondence to: F. D. Magalhães (E-mail: fdmagalh@fe.up.pt)

ABSTRACT: A functionalized fumed silica was dispersed in water using a nonionic surfactant, yielding a stable nanodispersion. This was blended with an aqueous acrylic polymer dispersion to produce hybrid nanocomposite films. The silica particles were shown to be well dispersed in the polymer matrix, with little agglomeration. Further evidence of good compatibility between the silica and acrylic polymer was given by the improved thermal stability of the nanocomposite compared with the pristine polymer. The nanocomposite films exhibited significantly lower dirt pick-up behavior, which seems to be associated to the nanoroughness of the composite film surface observed in AFM analysis. This decreases the contact area between film and micrometric dirt particles. Surface tension and hardness do not seem to be significantly different in the composite and noncomposite materials. This approach may provide a strategy to obtain hybrid coatings with self-cleaning properties, taking advantage of the relatively low cost, and large availability of fumed silica. © 2012 Wiley Periodicals, Inc. J. Appl. Polym. Sci. 000: 000–000, 2012

KEYWORDS: nanocomposite; fumed silica; acrylic polymer; self-cleaning; aqueous dispersion

Received 22 July 2011; accepted 27 February 2012; published online
DOI: 10.1002/app.37582

INTRODUCTION

Polymer nanocomposite materials have been shown to possess improved performances in terms of mechanical, thermal, or electrical properties, to name only a few.[1,2] In particular, applications of metal oxide nanoparticles, in particular nanosilica, in high-performance coating applications have been receiving significant attention.[3] Nanosilica is studied in this work as filler for waterborne acrylic polymer latex, having in mind application in façade paint formulations. This nanomaterial is commercially available in mainly two forms: colloidal and fumed (pyrogenic) silica, both with and without surface functionalization. Colloidal silica production is based on the Stöber method and is commercially available as a stable dispersion in different liquid media, including water. The particle size distributions are very homogeneous and tunable to different average sizes, ranging from tens to hundreds of nanometers. Fumed silica, on the other hand, is produced via flame hydrolysis and has primary particle sizes of $\sim$ 20 nm. Complete deagglomeration is not possible, but efficient dispersion in liquid media can yield agglomerates with dimensions lower than 100 nm. Dispersion in water leads to strong thixotropy at relatively low concentrations. This material is actually used as a rheological agent in waterborne coating formulations for this same reason. However, fumed silica has a significantly lower cost than colloidal silica, and thus our interest in exploring its potential as a nanofiller in waterborne composite coatings.

Incorporation of nanoparticles in aqueous latexes can follow two strategies: encapsulation in the polymer particles during the emulsion polymerization process or blending of the final latex with the nanoparticles, pre-dispersed in water or not. Several works report encapsulation of colloidal silica by *in situ* free-radical emulsion polymerization, using alcoxysilanes as surface modifiers for making the hydroxyl-rich silica surface compatible with the polymer matrixes. In particular, 3-methacryloxypropyltrimethoxysilane (MPS) has been used in many works for encapsulation with styrene or acrylic monomers.[4–7] In a distinct approach, Ding et al.[8,9] reported using oleic acid to make the surface of unfunctionalized colloidal silica organophilic, therefore achieving encapsulation with polystyrene and poly(methyl methacrylate). Bailly et al.[10] developed a method to graft

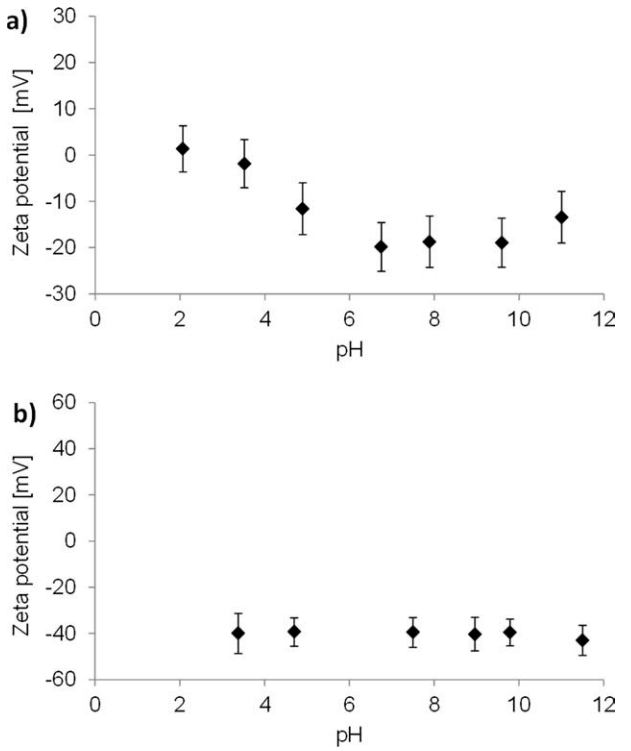

Figure 1. Zeta potential versus pH for nanosilica aqueous dispersions using (a) nonionic and (b) anionic surfactants.

alcoxyamine initiators on the surface of silica particles and subsequently grow polystyrene chains. Colloidal silica particles treated by this process were then encapsulated in polystyrene shells via miniemulsion polymerization. Barthet et al.[11] described a process to encapsulate unfunctionalized colloidal silica with co-polymers of 4-vinylpyridine (4VP) and acrylic monomers or styrene. This strategy takes advantage of the acid–base interactions of silica and (4VP), yielding stable dispersions. In most of the reported works, the dispersion medium for polymerization is a water/alcohol mixture to facilitate colloidal silica dispersion and stabilization.

Very little information is available on encapsulation of fumed silica in aqueous latexes.[12] Our own initial attempts indicated that encapsulation by *in situ* polymerization is a difficult task, the fumed silica (functionalized or not) tending to remain dispersed in the aqueous medium or adsorbed at the surface of the polymeric particles. Additional complications arise considering that in industrial applications, like waterborne coatings, the use of volatile organic cosolvents, often used to help dispersion, has to be minimized, and that the total solids content must be relatively high (typically 35%–65%).[13]

Encapsulation of inorganic nanoparticles in a polymer dispersion would be *a priori* considered the best strategy to form nanocomposite films from waterborne latexes, as the particles are "pre-dispersed" within the polymer matrix, and, after latex coalescence, particle agglomeration is minimized.[3] Nevertheless, Xiong et al.[14] have shown that simpler processes, involving high-energy blending of silica and polymer dispersions, can produce stable co-dispersions that yield homogeneous nanocomposite films with improved mechanical resistance. The silica contents tested, relative to solid content of original latex, were between 1 and 7 wt %.

In this article, we describe a process to obtain nanocomposite acrylic films with high silica content (24 wt %) from a blend of nanosilica and polymer dispersions. The films show good dispersion of the silica particles throughout the polymer matrix, without significant agglomeration. An acrylic latex was selected for its common use as a binder in exterior façade paints, which is the envisioned application for the nanocomposite coating. The fumed silica used has acrylate surface functionalization, which facilitates compatibility and promotes interaction with the polymer matrix.[3] The nanoparticles' hydrophobicity implied the use of an appropriate surfactant to ensure appropriate dispersion and stability in water. Note that dispersion of nonfunctionalized fumed silica in water would have been impossible for the concentrations used, due to strong viscosity increase due to interparticle hydrogen bonding.

The nanocomposite films obtained were characterized to evaluate the quality of the nanodispersion, surface topography, hardness, thermal stability, and dirt pick-up behavior. The good results obtained in terms of dirt pick-up indicate that this nanocomposite dispersion has potential use in façade paint formulations, where low retention of aerial dirt particles is relevant for preservation of the visual appearance of the coating.

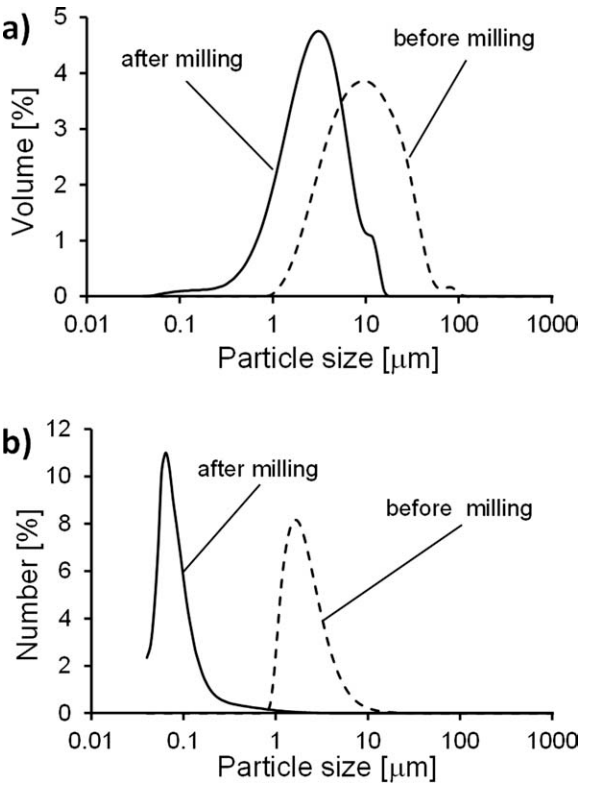

Figure 2. Volume (a) and number (b) particle size distributions for nanosilica dispersed in water with nonionic surfactant: before and after milling with glass spheres.

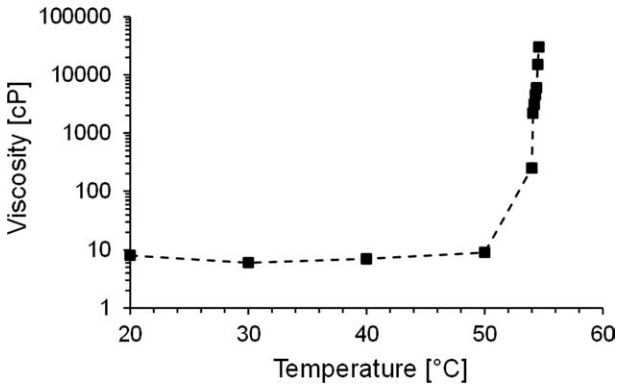

Figure 3. Effect of temperature in the viscosity of nanosilica dispersion when using nonionic surfactant. Silica concentration is 24 wt % and surfactant concentration is 5 wt %.

EXPERIMENTAL

Materials

The nanosilica used was a fumed silica functionalized with methacryloxypropyl-tri-methoxysilane (surface area = 150 ± 25 m^2/g, carbon content = 4.5–6.5 wt %, SiO_2 content based on ignited material = 99.8 wt %). The surfactants tested were an ethoxylated fatty alcohol nonionic surfactant and an alkyl aryl ether sulphate anionic surfactant. The polymeric dispersion was an acrylic resin based on acrylic and methacrylic acid esters, commonly used in waterborne façade paint formulations. Relevant properties are: solid content = 46% (typical value for latexes used in waterborne coatings), pH = 8.5, average particle size = 0.12 μm.

Dispersion of Nanosilica in Water and Combination with Acrylic Resin

The functionalized fumed silica used in this study is hydrophobic and a surfactant is needed for appropriate dispersion in water. The goal was defined as dispersing 24 wt %, which allows for an appropriate silica concentration on the final composite dry film. A minimum surfactant concentration of 5 wt % (based on final liquid dispersion weight) was identified for both anionic and nonionic surfactants, because at lower concentrations the dispersions were highly viscous. The final viscosities of the silica dispersions at this concentration were 30 cP with nonionic surfactant and 10 cP with anionic surfactant. In both cases, the pH of the final dispersions was approximately 7.

The surfactants were dissolved in water under intense stirring at 70°C, to accelerate dissolution. After cooling, the solutions remained perfectly clear and fluid, with no indication of surfactant insolubilization. These solutions were then charged onto a jacketed mill vessel and the nanosilica powder was gradually added. The silica was initially dispersed under 2500 rpm, for 15 min. A milling step, using 2-mm glass beads, was then performed to ensure effective silica deagglomeration, as discussed later. Stirring continued at 2500 rpm for 1–2 hr after adding the beads. The vessel was refrigerated so that the temperature in the liquid did not exceed 30°C. Finally, the glass beads were filtered out and the dispersion allowed resting for 24 hr to release air incorporated during the mixing process.

The nanosilica dispersion was then combined with the commercial polymer dispersion, to obtain a silica composition of 24 wt % relative to the final dry mass. Mixing of the two dispersions was performed with a Cowles impeller at 1000 rpm for 15 min.

Characterization Methods

The particle size distribution in the nanosilica dispersions was obtained with a Beckman Coulter LS230 (LS230) with a wet module. The measurement range goes from 0.04 to 2000 μm, using a Polarization Intensity Differential Scattering (PIDS) method. Rheology measurements were made with a Brookfield DV III Ultra, with different spindles for attaining torque between 10% and 90% at 100 rpm.

Water contact angles were measured using the static sessile drop method, on a Dataphysics OCA 20 goniometer, using distilled water as the reference liquid. Thermogravimetric analysis (TGA) was performed on a Netzsch – TG 206 F apparatus, under 20 mL min^{-1} N_2 flow and a heating rate of 20°C min^{-1}.

Dirt pick-up tests were performed separately with inorganic and organic ashes. These were spread over the film surface using a brush. Excess free ash was removed afterward. The surface was then washed under a controlled water stream (flow rate 10 mL s^{-1}) during 1.5 min. The color difference relative to the pristine (unexposed) surface, ΔE, was measured before and after washing, using a Gretag Macbeth Color-Eye 3100 spectrophotometer. Atomic force microscopy (AFM) and nanoindentation measurements were made in a Veeco Metrology Multimode - Nanoscope

Table I. Stability of Nanosilica Dispersion

				Particle size distribution (μm)			
Time	Sedimentation	Viscosity (cP)[a]	pH	Mean (Vol.)	SD (Vol.)	Mean (Num.)	SD (Num.)
1st day	No	40	6.7	1.16	0.73	0.08	0.06
1st week	No	277/198	6.8	1.01	0.96	0.07	0.04
2nd week	No	935/250	6.8	1.20	0.71	0.08	0.06
3rd week	No	1955/550	6.6	1.17	0.72	0.08	0.06
4th week	No	7000/1000	6.5	1.15	0.71	0.08	0.07

[a]The two values separated by a slash correspond to viscosities measured before and after manual mixing, respectively.

Applied Polymer SCIENCE

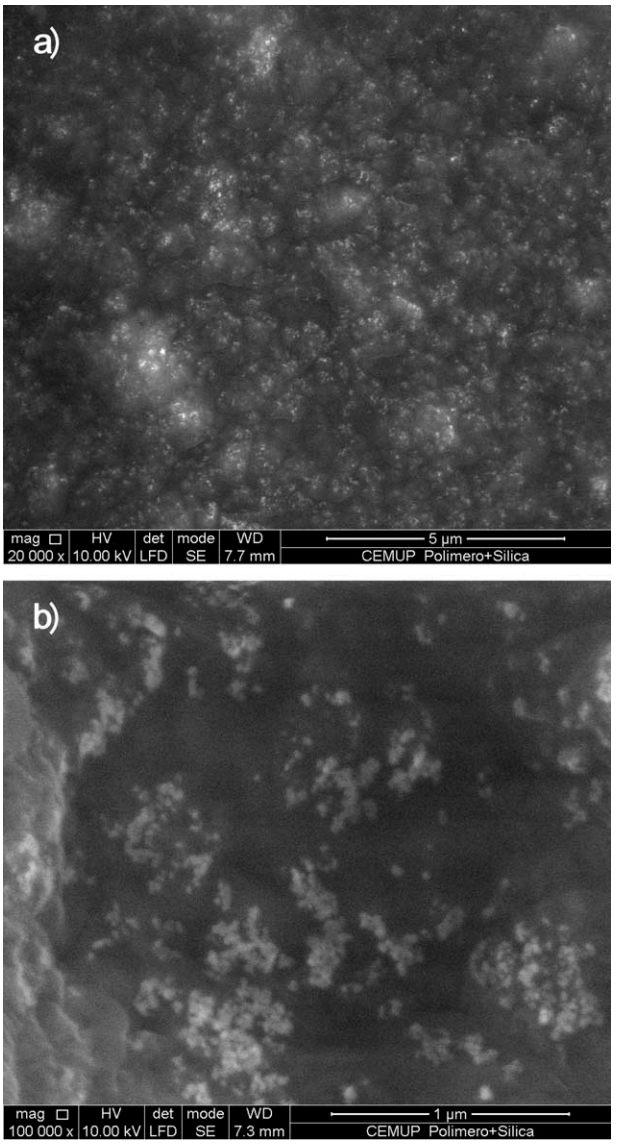

Figure 4. SEM image of dry nanocomposite film. Magnifications: (a) ×20000 and (b) ×100,000 (right).

IVA at CEMUP (Centro de Materiais da Universidade do Porto). Scanning electronic microscopy (SEM) analysis was performed at CEMUP using a JEOL JSM 35C - Noran Voyager equipment. Samples were coated with a gold/palladium alloy.

RESULTS AND DISCUSSION

Nanosilica Dispersion in Water

Figure 1 shows the Zeta potentials as a function of pH for dispersions of nanosilica in water using both types of surfactants. Despite the isoelectric point being attained at pH = 2 with the nonionic surfactant [Figure 1(a)], the dispersion remained always stable, due to the steric repulsion effect associated with this type of surfactants. On the other hand, the anionic surfactant yielded lower Zeta potential throughout the pH range tested.

After blending the silica dispersion stabilized with ionic surfactant with the acrylic latex, immediate precipitation occurred, probably due to interference between the surfactants systems used in the two dispersions. On the other hand, when using the nonionic surfactant the mixture remained stable and fluid. Silica dispersion with ethoxylated fatty alcohol was therefore adopted for most of the remaining work.

Glass sphere milling was a determinant step for obtaining good deagglomeration of silica in water. Figure 2 shows the volume and number particle size distributions for nanosilica dispersed in water with nonionic surfactant, before and after milling. It is noticeable that the mechanical stirring used in the initial dispersion is insufficient to obtain sufficient particle deagglomeration. Milling significantly reduces the average particle size. It must be noted that the volume distribution still indicates the presence of a significant fraction of agglomerates with micrometric dimensions. However, the number distribution shows that most of the particles are below the nanometric threshold of 100 nm. Note that submitting the dispersion to ultrasounds after mechanical stirring did not improve the size distributions. Milling was therefore used in all preparations.

Interestingly, the silica dispersion shows a very steep increase in viscosity as temperature reaches about 50°C, as shown in Figure 3, occurring gel formation. This is a reversible process: after decreasing the temperature the dispersion recovers the original viscosity and particle size distribution. This gelling effect may be associated to temperature-induced surfactant desorption from the silica surface, allowing for the onset of strong interparticle interactions. This is not a relevant

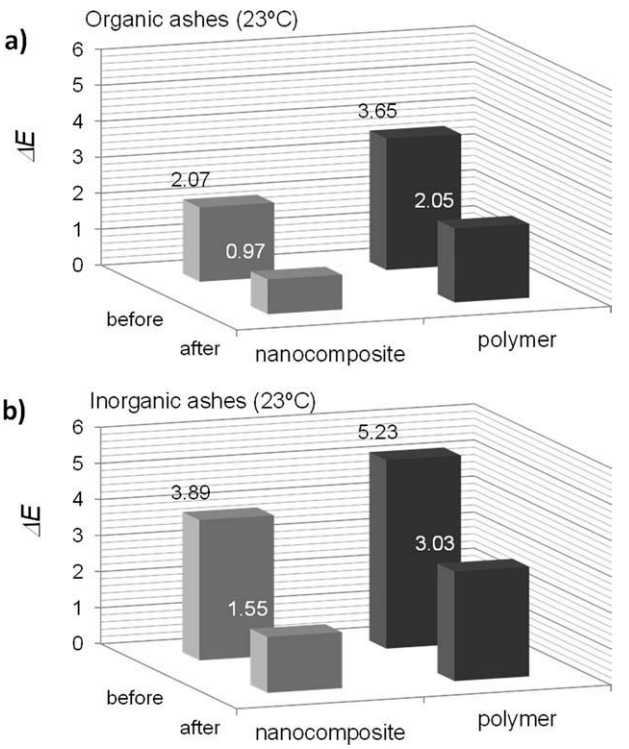

Figure 5. Organic (a) and inorganic (a) ash retention, before and after washing with water, for the pristine acrylic resin and nanocomposite dry films.

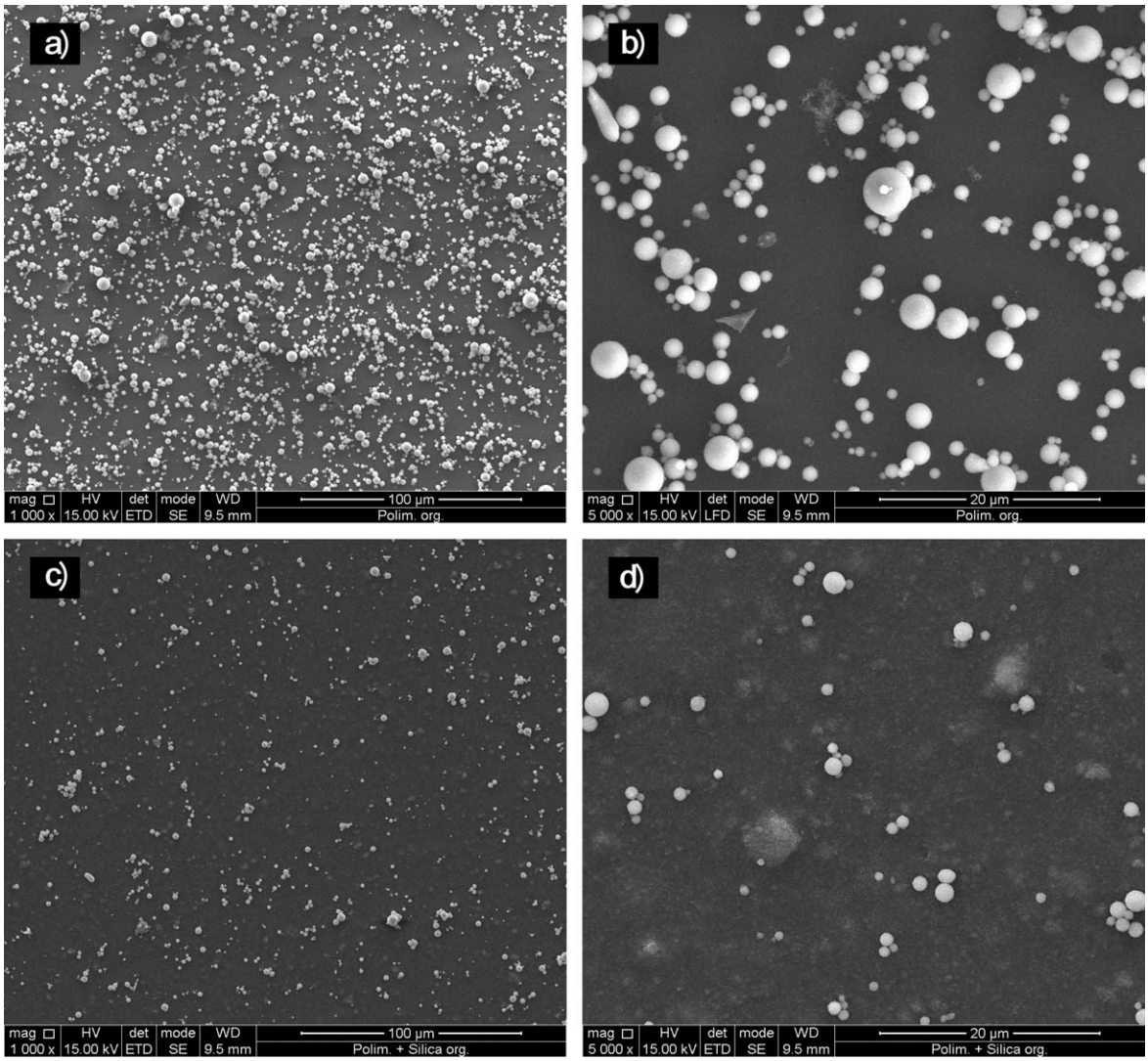

Figure 6. SEM images of surfaces after exposure to organic ashes and subsequent washing. The two images on top [(a) and (b)] show the pristine acrylic resin film and the two on bottom [(c) and (d)] show the nanocomposite film.

limitation for the process under study, because silica dispersion is performed under forced cooling, avoiding overheating above 50°C. This temperature dependence was not present when the ionic surfactant was used, the viscosity remaining constant up to 70°C.

This dispersion acquires a thixotropic character after resting for some days, but rapidly regains the original fluidity after agitation. This raises questions concerning the stability of the dispersion along time. To clarify this issue, the viscosity and particle size distributions of a dispersion maintained at 23°C in the dark were measured weekly along 1 month (Table I). Viscosity was measured before and after manual stirring, to evaluate the thixotropic character of the liquid. The results show that pH and particle size distribution did not change along this experiment. However, thixotropy increases significantly. After manual stirring, viscosity decreases but the original viscosity is not recovered. No visible sedimentation was observed during the test period. The increasing thixotropy of the dispersion with time indicates that it should be used within a couple of weeks after production, to facilitate processing.

Nanosilica Distribution in Composite Film

Acrylic polymer films incorporating nanosilica were obtained by casting and drying the blended aqueous dispersions described before. The silica content in the films, relative to the final dry mass, was 24% (w/w). SEM images of these composite films are shown in Figure 4. Thanks to polymer chain mobility, latex coalescence yielded a uniform dry film that envelope the silica nanoparticles. These, seen as white dots in the images, are well distributed throughout the polymer matrix. The nanometric character of the silica seems to be generally preserved in the composite material, as primary particles (~ 20 nm in diameter) can be individually identified. The morphology of the particle distribution observed in the polymer matrix is characteristic of fumed silica nanocomposites. An example is found in the work of Zhou and Gu for solvent-based blends of fumed silica with polyurethane-acrylic coatings.[15]

Applied Polymer SCIENCE

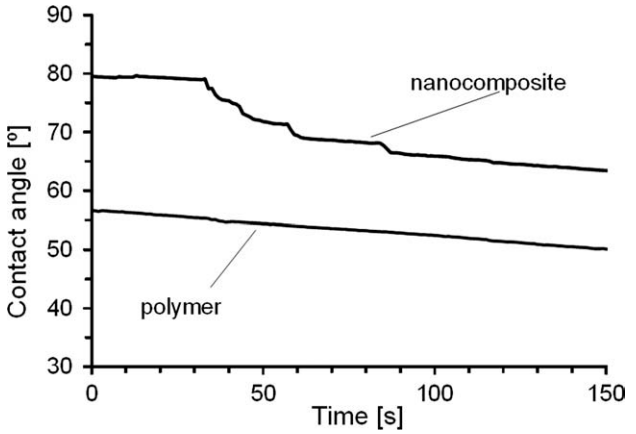

Figure 7. Water contact angle for of pristine acrylic resin and nanocomposite films.

Dirt Pick-up

In the evaluation of dirt pick-up behavior, the retention of organic and inorganic ashes at the surface is measured by spectrophotometry, before and after washing with running water. The results are presented in Figure 5. For both kinds of ash, the dirt pick-up is significantly lower for the nanocomposite surface, both before and after washing. These results are confirmed by the SEM images of the surfaces after washing (Figure 6). The presence of a much higher amount of dirt particles on the non-composite surface [Figure 6(a,b)] is evident. It can therefore be concluded that the composite surface exhibits self-cleaning behavior, with low tendency to retain dirt particles and easy dirt removal ability by running water, which simulates the action of rainfall.

Water Contact Angle

The water contact angles were measured along time on the film surface. The results, shown in Figure 7, indicate that the nanocomposite is more hydrophobic than the original acrylic resin. This difference is not substantial and cannot, by itself, justify the significantly lower dirt pick-up of the composite surface. The irregular decrease in contact angle observed for the nanocomposite may be associated to the irregularity of the surface, as discussed later.

Surface Topography

The surface topography of the nanocomposite and pristine acrylic resin films was analyzed by AFM. In Figure 8, the dry

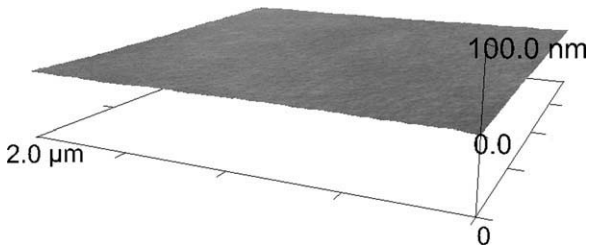

Figure 8. AFM 3D image of 2 × 2 μm surface of pristine acrylic resin film.

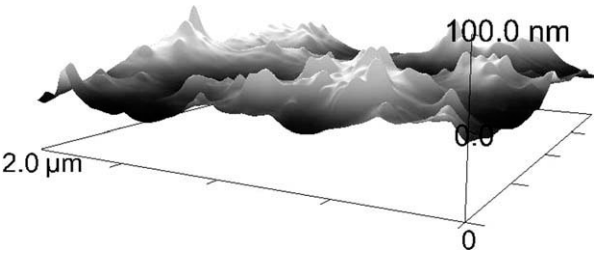

Figure 9. AFM 3D image of 2 × 2 μm surface of nanocomposite film.

polymer film presents a very smooth topography, seen as a very flat surface. On the other hand, the nanocomposite film (Figure 9) shows significant roughness on a nanometric scale. Topographic top-views of the two surfaces are shown in Figure 10, further illustrating the strong difference between the two films.

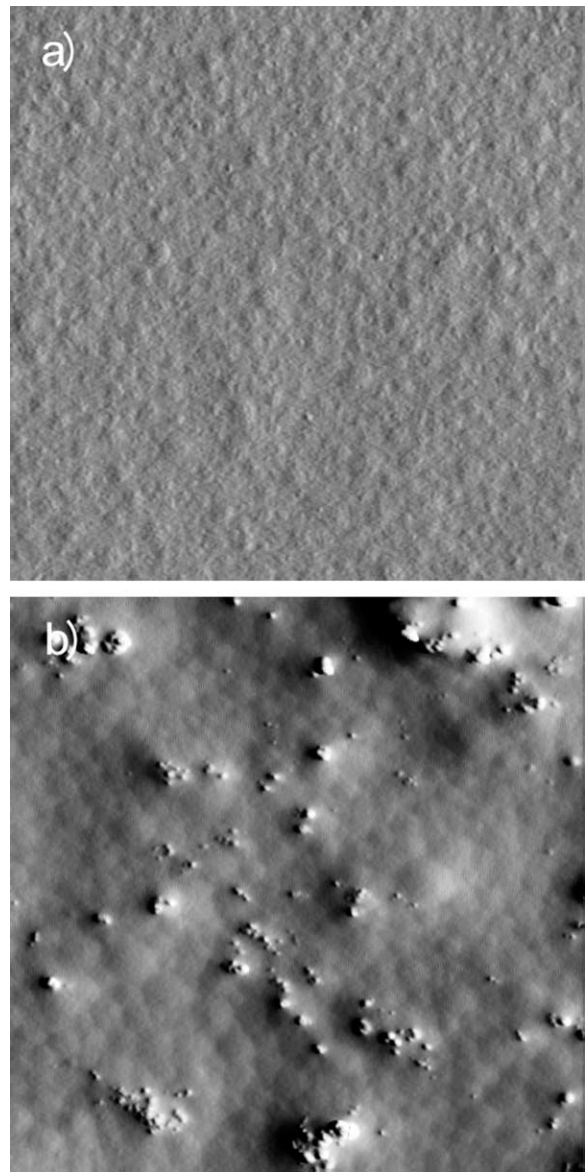

Figure 10. Topographic image of pristine acrylic resin (a) and nanocomposite (b) surfaces, 2 × 2 μm, obtained by AFM analysis.

Table II. Surface Hardness Results Determined by Nanoindentation

	Acrylic polymer film Hardness (MPa)	Nanocomposite film Hardness (MPa)
Mean	215	196
SD	48	19

This feature may be the main cause for the lower dirt pick-up of the nanocomposite film, because the surface area available for contact and adhesion to aerial dirt particles (sized in the micrometer range) is significantly reduced.

Surface Hardness

The tackiness and surface hardness of a polymeric film are both a function of chain segment mobility.[16] On a harder surface, adhesive molecular interactions are expected to be less intense, and colliding airborne dirt particles will more easily bounce off the surface. It is therefore relevant to investigate whether the presence of a nanofiller increases surface hardness, indicating hindered molecular mobility and decreased tackiness. The surface hardness of the filled and unfilled polymer films was measured by nanoindentation. Table II shows that the two materials cannot be distinguished in terms of hardness. This cannot therefore be accounted as a determinant property for the self-cleaning character of the nanocomposite surface.

Thermal Stability

The thermal degradation behavior under inert conditions is often used as an evaluation of the quality of nanocomposite materials. Figure 11 shows the thermogravimetric curves obtained for the neat acrylic resin and the nanocomposite. Incorporation of nanosilica increased thermal stability significantly—the inflexion point in the weight loss curve shifted by 19°C. This is an indication of good nanoparticle dispersion and strong interaction with the polymer matrix.[17,18]

Effect of Temperature on Dirt Pick-up

To evaluate the effect of temperature on the nanocomposite and pristine resin surfaces, films of both materials were placed in an oven at 60°C during 30 min for thermal stabilization. Afterward, the surfaces were pulverized with ashes, still inside the oven. The spectrophotometric procedure described before for analyzing dirt pick-up was them followed. Figure 12 shows the results obtained. Ash retention increased significantly in both materials, both before and after washing, and now there are is no difference between the nanocomposite and unfilled polymer materials. At this high temperature, the increased tackiness of the thermoplastic acrylic polymer becomes the preponderant factor, determining surface behavior. It must be noted that, after cooling the films back to ambient temperature, the original dirt pick-up performance is recovered. AFM topography analyses of the cooled surfaces (not shown here) also showed no changes in relation to the original topography [Figures 9 and 10(b)].

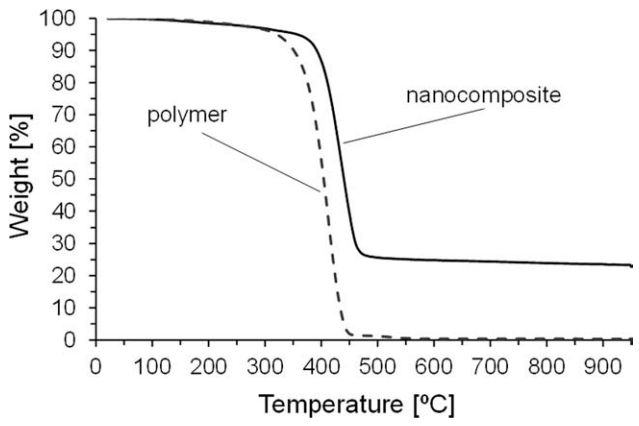

Figure 11. Thermal gravimetric analysis results for pristine acrylic resin (dashed line) and nanocomposite (continuous line) materials.

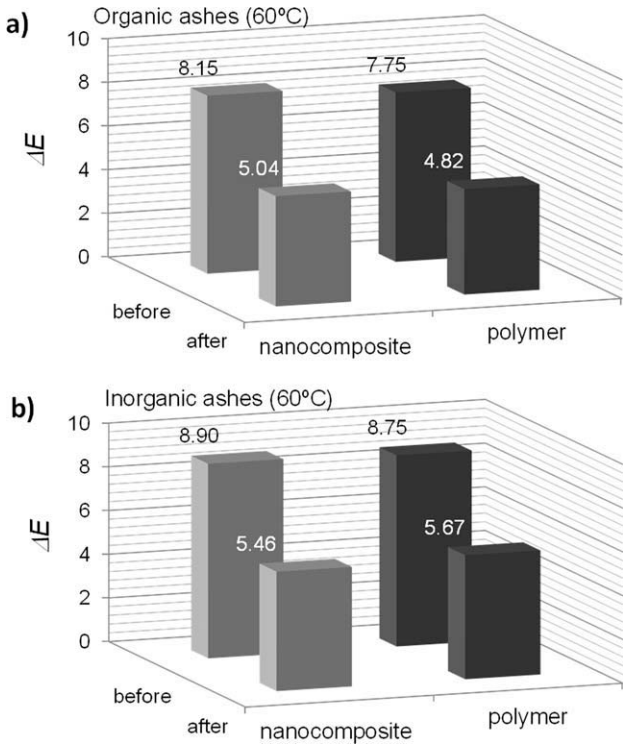

Figure 12. Organic (a) and inorganic (b) ash retention at 60°C before and after washing with water.

CONCLUSIONS

A stable dispersion was obtained by high energy blending of an acrylic polymer latex with an acrylate-functionalized fumed silica predispersed in water using an appropriate surfactant. The dry films produced showed homogeneous distribution of silica particles, preserving the nanometric character. The thermal stability of the nanocomposite was higher than for the pristine acrylic polymer. It was concluded that dispersion blending was a valid strategy for obtaining nanocomposite films from aqueous latexes containing fumed silica, without need for more complex encapsulation of the nanoparticles in the polymerization process.

The nanosilica-filled films exhibit significantly lower dirt pick-up behavior when compared with the pristine polymer. This seems to be associated with the nanoroughness of the composite film surface, confirmed by AFM analysis, which decreases the

contact area between the film and dirt particles. Surface tension and hardness do not seem to be significantly different surface in the two materials. The dirt pick-up performance of the nanocomposite worsens significantly when the surface temperature is increased to 60°C, becoming identical to the pristine polymer, due to increased tack surmounting the nanoroughness effect. However, the original performance is recovered when the surface cools down.

The approach followed to obtain nanocomposite films, based on high-energy blending of inorganic and organic aqueous dispersions, may be an economical and straightforward approach to produce hybrid coatings with self-cleaning properties, taking advantage of the relatively low cost, and large availability of fumed silica. The beneficial effects of incorporating this nanocomposite film-forming dispersion on a façade paint formulation are currently under study.

ACKNOWLEDGMENTS

Funding for this work was provided by FCT - Fundaç ão para a Ciência e Tecnologia (project PTDC/EQU-EQU/65300/2006), and by FEDER/QREN (project RHED) in the framework of Programa Operacional Factor de Competitividade -COMPETE. Catarina Carneiro thanks FCT for PhD grant SFRH/BDE/15569/2005.

REFERENCES

1. Hussain, F.; Hojjati, M.; Okamoto, M.; Gorga, R. E.; *J. Compos. Mater.* **2006,** *40*, 1511.
2. Paul, D. R.; Robeson, L. M. *Polymer* **2008,** *49*, 3187.
3. You, B.; Wen, N.; Cao, Y.; Zhou, S.; Wu, L. *Polym. Int.* **2009,** *58*, 519.
4. Bourgeat-Lami, E.; Jacques Lang, J. *J. Colloid Interface Sci.* **1999,** *289*, 281.
5. Yua, Y.-Y.; Chena, C.-Y.; Chen, W.-C. *Polymer* **2003,** *44*, 593.
6. Zhu, A.; Shi, Z.; Cai, A.; Zhao, F.; Liao,T. *Polym. Test.* **2008,** *27*, 540.
7. Zhu, A.; Cai, A.; Zhou, W.; Shi, Z. *Appl. Surface Sci.* **2007,** *254*, 3745.
8. Ding, X.; Zhao, J.; Liu, Y.; Zhang, H.; Wang, Z. *Mater. Lett.* **2004,** *58*, 3126.
9. Ding, X.; Wang, Z.; Han, D.; Zhang, Y.; Shen, Y.; Niu, L. *Nanotechnology* **2006,** *17*, 4796.
10. Bailly, B.; Donnenwirth, A.-C.; Bartholome, C.; Beyou, E.; Bourgeat-Lmi, E. *J. Nanomater.* **2006**, *2006*, doi:10.1155/JNM/2006/76371.
11. Barthet, C.; Hickey, A.; Cairns, D.; Armes, S. *Adv. Mater.* **1999,** *3*, 1998.
12. Mahdavian, A. R.; Ashjari, M.; Makoo, A. B. *Polymer* **2007,** *43*, 336.
13. Lovell, P. A.; El-Aasser, M. S., Eds. Emulsion Polymerization and Emulsion Polymers. Wiley: New York, **1997;** p 630.
14. Xiong, M.; Wu, L.; Zhou, S.; You, B. *Polym. Int.* **2002,** *51*, 693.
15. Zhou, S.; Gu, G. *Physics* **2004,** *9*, 1593.
16. Istaván Benedek. Pressure Sensitive Formulation. VSP BV, Zheist, **2000;** p. 68.
17. Yang, F.; Nelson, G. L. *Polym. Adv. Technol.* **2006,** *17*, 320.
18. Zeng, R.; Rong, M. Z.; Zhang, M. Q.; Liang, H. C.; Zeng, H. M. *J. Mater. Sci. Lett.* **2001,** *20*, 1473.